Protein–RNA Cross-Linking in the Ribosomes of Yeast under Oxidative Stress

ARTICLE *in* JOURNAL OF PROTEOME RESEARCH · JANUARY 2007

Impact Factor: 4.25 · DOI: 10.1021/pr060337l · Source: PubMed

research articles Journal of proteome research

Protein−RNA Cross-Linking in the Ribosomes of Yeast under Oxidative Stress

Hamid Mirzaei and Fred Regnier*

Department of Chemistry, Purdue University, West Lafayette, Indiana 47907

Living systems have efficient degradative pathways for dealing with the fact that reactive oxygen species (ROS) derived from cellular metabolism and the environment oxidatively damage proteins and DNA. But aggregation and cross-linking can occur as well, leading to a series of problems including disruption of cellular regulation, mutations, and even cell death. The mechanism(s) by which protein aggregation occurs and the macromolecular species involved are poorly understood. In the study reported here, evidence is provided for a new type of aggregate between proteins and RNA in ribosomes. While studying the effect of oxidative stress induced in the yeast proteome it was noted that ribosomal proteins were widely oxidized. Eighty six percent of the proteins in yeast ribosomes were found to be carbonylated after stressing yeast cell cultures with hydrogen peroxide. Moreover, many of these proteins appeared to be cross-linked based on their coelution patterns during RPC separation. Since they were not in direct contact, it was not clear how this could occur unless it was through the RNA separating them in the ribosome. This was confirmed in a multiple-step process, the first being derivatization of all carbonylated proteins in cell lysates with biotin hydrazide through Schiff base formation. Following reduction of Schiff bases with sodium cyanoborohydride, biotinylated proteins were selected from cell lysates with avidin affinity chromatography. Oxidized proteins thus captured were then selected again using boronate affinity chromatography to capture vicinal diol-containing proteins. This would include proteins cross-linked to an RNA fragment containing a ribose residue with 2′,3′-hydroxyl groups. Some glycoproteins would also be selected by this process. LC/MS/MS analyses of tryptic peptides derived from proteins captured by this process along with MASCOT searches resulted in the identification of 37 ribosomal proteins that appear to be cross-linked to RNA. Aggregation of proteins with ribosomal RNA has not been previously reported. The probable impact of this phenomenon cells is to diminish the protein synthesis capacity.

Keywords: Proteomics • oxidative stress • hydrogen peroxide • yeast • biotin hydrazide • avidin affinity chromatography • boronate affinity chromatography • protein fragmentation • protein cross-linking • ribosomal proteins • protein−RNA cross-linking • tandem mass spectrometry • protein identification

Introduction

Reactive oxygen species (ROS) are at the heart of a series of oxidative stress diseases and aging.[1−3] Although cells frequently encounter environmental ROS and even generate ROS during normal cellular metabolism, excessive amounts of ROS can irreversibly oxidize proteins. These oxidized proteins are generally recognized and channeled to proteasomes for degradation. But under excessive oxidative stress, proteasomes often loose their degradative efficiency. This loss of proteasomal function is believed to be due several phenomena. One is the intermolecular association of proteins, ostensibly through Schiff base formation but oxidatively induced changes in protein conformation may play a role as well.[4,5] The second is that these aggregated proteins are poor proteasome substrates. This leads to the accumulation of nongenetically coded, oxidative stress-induced protein aggregates that are quite different than genetically coded protein aggregates found in the interactome.

Oxidative stress is known to induce protein−DNA cross-linking.[6] Protein-DNA cross-linking has been implicated in cancer, immune system decline, cardiovascular disease, and neurological disorders.[2, 3, 7] Cross-linking can be initiated by oxidation of either proteins or DNA but has not been studied systematically using modern proteomic methods. In either case, cross-linking is most likely to occur when a protein is in a fixed position relative to a DNA strand, such as in histones or in the regulation of transcription.[8−11] Exact sites of protein−DNA cross-linking have only been examined in a few cases where interaction sites were the focus of an investigation.[12−15]

Oxidative stress-induced protein aggregation occurs through multiple mechanisms.[16] One is through Schiff base formation in which a carbonyl group on an oxidized protein reacts with a primary amine on a second protein. Another is through

* Corresponding author. E-mail: fregnier@purdue.edu.

intermolecular disulfide bond formation between proteins. Free radical cross-linking of proteins through carbon−carbon bond formation between tyrosine residues is yet another mechanism.[17] Free radical cross-linking probably also plays a role in protein−DNA cross-linking although the exact mechanism has not be determined. Protein aggregation can even be caused by the binding of degradative products of sugars and lipids to proteins.[18] Finally there is noncovalent aggregation. In this case, conformation changes resulting from oxidation expose hydrophobic and electrostatic domains at the surface of a protein that drive noncovalent aggregation.

It is becoming increasingly clear that oxidative stress-induced formation of both protein−protein and protein−DNA complexes are a problem for cells. It is seen in the case of neurodegenerative diseases[19] and physiological aging[3] that protein−protein aggregates, or aggresomes as they are sometimes called, diminish cellular viability and are of substantial toxicity, even to the point of causing cell death.[20] One of the most lethal aggregates is protein fibrils. Protein fibril formation, as seen in Alzheimer's disease (AD), is a noncovalent process thought to be related to conformational alteration resulting from the oxidation of protein.[21] These conformational changes expose small fibril forming domains that lead to intermolecular aggregation and the production of huge fibrils that often result in cell death.[1] Protein−DNA cross-lining is also a serious problem for cells, but of a different type. In this case the effect is either to compromise regulation or cause mutations.

The studies reported here describe the formation of a new type of oxidatively induce intermolecular complex, protein−RNA conjugates. During the course of excessive oxidative stress in yeast it was observed that ribosomal proteins were the most likely class of proteins to be oxidized and that many were covalently linked to RNA in close proximity within the ribosomal matrix.

Materials and Methods

Materials. Biotin hydrazide, ultralinked immobilized monomeric avidin, D-biotin, sodium cyanoborohydride, trifluoroacetic acid (TFA), Slide-A-Lyzer dialysis cassettes, and Coomassie blue (Bradford) protein assay kits were purchased from Pierce (Rockford, IL). Iodoacetamide, dithiothreitol (DTT), trypsin, glycerol, 2-mercaptoethanol, ethylenediaminetetraacetic acid (EDTA), HEPES buffer, Tris buffer, IGEPAL CA-630 nonioninc detergent, and *N*-α-tosyl-L-lysine chloromethyl ketone (TLCK) were obtained from Sigma Chemical Co. (St. Louis, MO). Sodium phosphate, urea, sodium chloride, magnesium chloride, and calcium chloride were purchased from Mallinkrodt (St. Louis, MO). Protease inhibitor cocktail was purchased from Roche Diagnostics (Indianapolis, IN). Ribonuclease I, from *E. coli*, was purchased from Fermentas (Hanover, MD). ZipTip pipet tips were purchased from Millipore Corporation (Bedford, MA). A Vydac 208TP54 reversed-phase C_8 column was purchased from W. R. Grace & Co (Columbia, MD). Coated nanospray tips were purchased from New Objective, Inc. (Woburn, MA). A TSK boronate 5PW column was purchased from Tosoh Biosciences (Montgomeryville, PA). DE44G00621 Zorbax 300SB-C18 reversed-phase column (75 μm × 150 mm) was purchased from Agilent Technologies, Inc. (Palo Alto, CA). Affinity selection and reversed-phase chromatographic (RPC) analyses were done on an Integral Micro-Analytical Workstation (Framingham, MA). The LC system used in conjunction with the mass spectrometer was an Agilent 1100 series instrument from Agilent Technologies, Inc (Palo Alto, CA). Mass spectral analyses were achieved using a PE Sciex QSTAR hybrid LC/MS/MS Quadrupole TOF mass spectrometer (Framingham, MA). All spectra were obtained in the positive ion mode.

Methods. Yeast Strain and Culture Conditions. The method of Yoo et al.[22] was followed in growing *Saccharomyces cerevisiae* wild-type strain SM1058.[23] Cells were grown at 37 ∀C in yeast extract-peptone-dextrose (YPD) medium (1% yeast extract, 2% peptone, 2% glucose) using a shaking incubator at 200 rpm. Cell growth was determined by optical density (OD) measurements at 600 nm. For processing a mid-log phase culture, overnight cultured cells were inoculated in fresh medium to a cell density of 0.2−0.3 OD_{600}.

Preparation of Total Protein from Yeast Treated with Hydrogen Peroxide. Exponentially growing cells at a density of 2.4 OD_{600} were treated with 5 mM hydrogen peroxide to induce oxidative stress (This concentration of hydrogen peroxide is sublethal and only decreases cell growth rate for a short period of time after which the cell resumes normal growth).[22] Cells from 50 or 500 mL cultures were harvested 1 h after addition of hydrogen peroxide and then washed twice with cold water by centrifugation at 3000 rpm for 10 min at 4 ∀C. The pellet was resuspended in lysis buffer (pH 7.4) containing 3.8 mM $NaH_2PO_4{\cdot}6H_2O$, 49.4 mM $Na_2HPO_4{\cdot}6H_2O$, 48.4 mM NaCl, 5 mM KCl, 20% glycerol, 1% 2-mercaptoethanol, 0.3% IGEPAL CA-630 (Sigma) nonionic detergent, complete-mini protease inhibitor, and 5 mM biotin hydrazide. After 30 min an equal volume of 30 mM sodium cyanoborohydride in lysis buffer was added to reduce C═N bonds. Cells were broken by repeated vortexing at 4 ∀C for 10 min with an equivalent volume of glass beads (0.6 mm diameter; Sigma, G-8772). Supernatant was collected by centrifugation at 14000 rpm for 10 min at 4 ∀C. Protein concentration was measured by the Bradford method using a Coomassie protein assay kit (Pierce). The final supernatant was kept for further processing.

Avidin Affinity Selection. Ultralinked immobilized monomeric avidin was packed into a stainless steel column (4.6 i.d. × 100 mm, 1.7 mL volume) at 100 psi. The packed column was washed with ten column volumes of phosphate-buffered saline (PBS) (0.1 M sodium phosphate, 0.15 M NaCl, pH 7.4) and five column volumes of biotin blocking and elution buffer (2 mM D-biotin in PBS) to block any nonreversible biotin-binding site on the column. Biotin from reversible biotin binding sites was removed by washing with five column volumes of regeneration buffer (0.1 M glycine, pH 2.8). Finally, the column was re-equilibrated with ten column volumes of PBS. Five hundred microliters of sample (2 mg/mL) followed by 0.25 mL of PBS was loaded into the column. The column was incubated at room temperature for 1 h and washed with ten column volumes of PBS to remove all unbound proteins. Biotinylated proteins were eluted with ten column volumes of biotin blocking and elution buffer, and the column was regenerated with ten column volumes of column regeneration buffer followed by ten column volumes of PBS.

Reversed-Phase Separation of Biotinylated Proteins. A Vydac 208TP54 reversed-phase C_8 column (7.9 mm × 250 mm) was used to desalt and fractionate biotinylated proteins. The reversed-phase column was equilibrated with five column volumes of buffer A (99.5% deionized H_2O (dI H_2O), 0.5% acetonitrile (ACN), and 0.1% TFA). Urea (6 M) was added to further denature the selected proteins before application to the reversed-phase column. After a five column volume wash a linear 60 min gradient was applied from 100% buffer A to 60% buffer B (5% dI H_2O, 95% ACN and 0.1% TFA) to elute proteins

from the column. A total of 27 fractions were collected. Collected fractions were vacuum-dried and stored for digestion.

Proteolysis. Six molar urea and 10 mM dithiothreitol were added to proteins fractions. After 1 h incubation at 65 ∀C, iodoacetamide was added to a final concentration of 10 mM and the reaction allowed to proceed for an additional 30 min at 4 ∀C. Samples were then diluted 6 fold by addition of 50 mM HEPES (pH 8.0) in 10 mM $CaCl_2$. Sequence grade trypsin (2%) was added and the reaction mixture incubated at 37 ∀C for at least 8 h. Proteolysis was stopped by addition of tosyl lysine chloroketone (TLCK) at a 1:1 (w/w) ratio.

Mass Spectrometry of Digested Fractions. The nanospray ionization mode was used to examine column fractions. Trypsin-digested fractions were desalted using Millipore Zip-Tips. Desalted digests were loaded into coated nanospray tips. Nanospray ionization was achieved at 1200 V with 25 units of curtain gas. Collision energy was adjusted for each peptide according to its m/z to yield comprehensive fragmentation. After acquisition of MS spectral data, MS/MS data were submitted to MASCOT for database searches and identification of the corresponding peptides and proteins. Analyst software version 1.0 of MASCOT was used to create the peak list from a raw data. No smoothing of the data, signal-to-noise ratio, or peak deisotoping was applied. Charge states were determined manually and specified during a MASCOT search for each peptide. The centroid of MS/MS peaks was determined using the following parameters. The merge distance was set at 100 ppm with minimum and maximum widths of 10 and 500 ppm, respectively. The percentage height was set at 50%, and the on-line version of MASCOT was used for all searches. Peptides were searched individually. The following search parameters were used for peptide identification: Database: NCBInr, taxonomy: *Saccharomyces cerevisiae* (72412 entries), enzyme: trypsin, missed cleavages: four, fixed modification: carboxymethylation of cysteine, peptide tolerance ± 1.2 Da, MS/MS tolerance ± 0.6 Da, peptide charge was specified for each peptide, monoisotopic peaks were used for identification. The MASCOT scoring system was used as a measure of identification certainty. A detailed description of the peptide scoring system used by MASCOT can be found @ http://www.matrixscience.com/help/scoring_help. The score threshold was adjusted to a 5% rate of false positives.

Boronate Affinity Chromatography. Proteins eluted from the avidin affinity column were dialyzed to exchange the buffer to boronate affinity column loading buffer (50 mM HEPES, 20 mM $MgCl_2$ pH 8.00). The boronate affinity column was equilibrated with ten column volumes of loading buffer and operated at 4 ∀C using a water jacket. After the protein fraction was administered, unbound proteins and salts were washed from the column with ten column volumes of loading buffer. The water jacket was removed, and the bound proteins were eluted using 50 mM Tris (competing diol), 40 mM EDTA (divalent cation) at pH 5.00. The eluted protein fraction was collected and further fractionated on the Vydac C_8 reversed-phase column. Fractions collected from the reversed phase column were individually digested as previously described.

Digestion with Ribonuclease I. Ribonuclease I was added to fraction collected from the C_8 reversed-phase column after tryptic digestion. It is critical to note that a 1:1 (w/w) ratio of TLCK inhibitor was added after trypsin digestion to inhibit proteolysis of ribonuclease. The buffer used was the same buffer for tryptic digestion (50 mM Tris pH 8.00, 0.7 M urea). Ribonuclease I was reconstituted in 50 mM Tris (pH 8.00), 100 mM NaCl, 0.01% Triton X-100, and 50% glycerol (final concentration 10u/μL). One microliter of reconstituted ribonuclease I from *E. coli* was added to each digested protein fraction for 4 h at 37 ∀C.

LC/MS Analysis. Peptides derived from protein fractions collected from the Vydac C8 column were analyzed using an Agilent 1100 series HPLC- PE Sciex QSTAR hybrid LC/MS/MS Quadrupole-TOF mass spectrometer. Peptide mixtures were separated on an Agilent Zorbax C_{18} column (75 μm × 150 mm) using an Agilent 1100 series instrument (Agilent Technologies, Inc. Palo Alto, CA) at 0.2 μL/min. Solvent A was 0.01% TFA in deionized H_2O (dI H_2O), and solvent B was 95% CH_3CN/0.01% TFA in dI H_2O. Flow from the column was directed to the QSTAR workstation (Applied Biosystems, Framingham, MA) equipped with an ESI source. Peptides were separated in a 60 min linear gradient (from 0% B to 60% B). MS/MS spectra were obtained in the positive ion mode, 5400 V of ionization voltage, 30 units of curtain gas at a sampling rate of one spectrum per second.

MASCOT Search. MASCOT searches of LC/MS/MS spectra were conducted against bakers' yeast (*S. cerevisiae*) database. Variables were set exactly the same as in the previous case except that amino acids cross-linked to nucleotide were also included as variable modifications. According to the literature, these amino acids include arginine cross-linked to guanine, tyrosine cross-linked to cytosine, lysine cross-linked to guanine, and serine and threonine cross-linked to guanine (Appendix 2).

Results

The study reported here was part of a larger study directed at the identification of proteins that are carbonylated as a result of oxidative stress. Proteins from lysates of H_2O_2-stressed yeast cultures were derivatized with biotin hydrazide, reduced with sodium cyanoborohydride, and after dialysis were applied to an avidin affinity chromatography column. After being washed with PBS buffer to remove nonadsorbed proteins, bound proteins were eluted (Figure 1a). Since affinity selection was carried out using a nondenaturing buffer, non-biotinylated proteins would also be selected if they were covalently or noncovalently associated with biotinylated proteins. Proteins captured by the avidin column were eluted from the affinity column with a biotin displacer and fractionated on a Vydac C_8 reversed-phase chromatography (RPC) column (Figure 1b). The RPC fractions were then digested with trypsin and analyzed by nanospray ionization-mass spectrometry (Nano-ESI-MS) (Figure 1c).

Roughly 400 proteins from the nucleus (nucleoplasm, nucleolus, nuclear chromosomes, and nuclear chromatin), mitochondria (outer membrane bound), cytoplasm, Golgi apparatus, ribosomes, proteasomes, endoplasmic reticulum, incipient bud sites, spliceosomes, plasma membranes, cytoplasmic microtubules, endosomes, and vacuolar membrane were identified in the initial report of this work.[24] Although the proteins identified were from a diverse group of cellular organelles, more proteins were identified from ribosomes than any other organelle. In fact, 85% of the proteins in the yeast ribosome were selected by this method. Clearly proteins in the ribosome were a major target.[24] This paper focuses on a deeper investigation of protein oxidation in ribosomes during oxidative stress.

Sixty-six ribosomal proteins were detected in the 27 fractions collected (Figure 1b) from the C_8 reversed-phase column based on manual MS/MS sequencing of 1192 peptide peaks. This

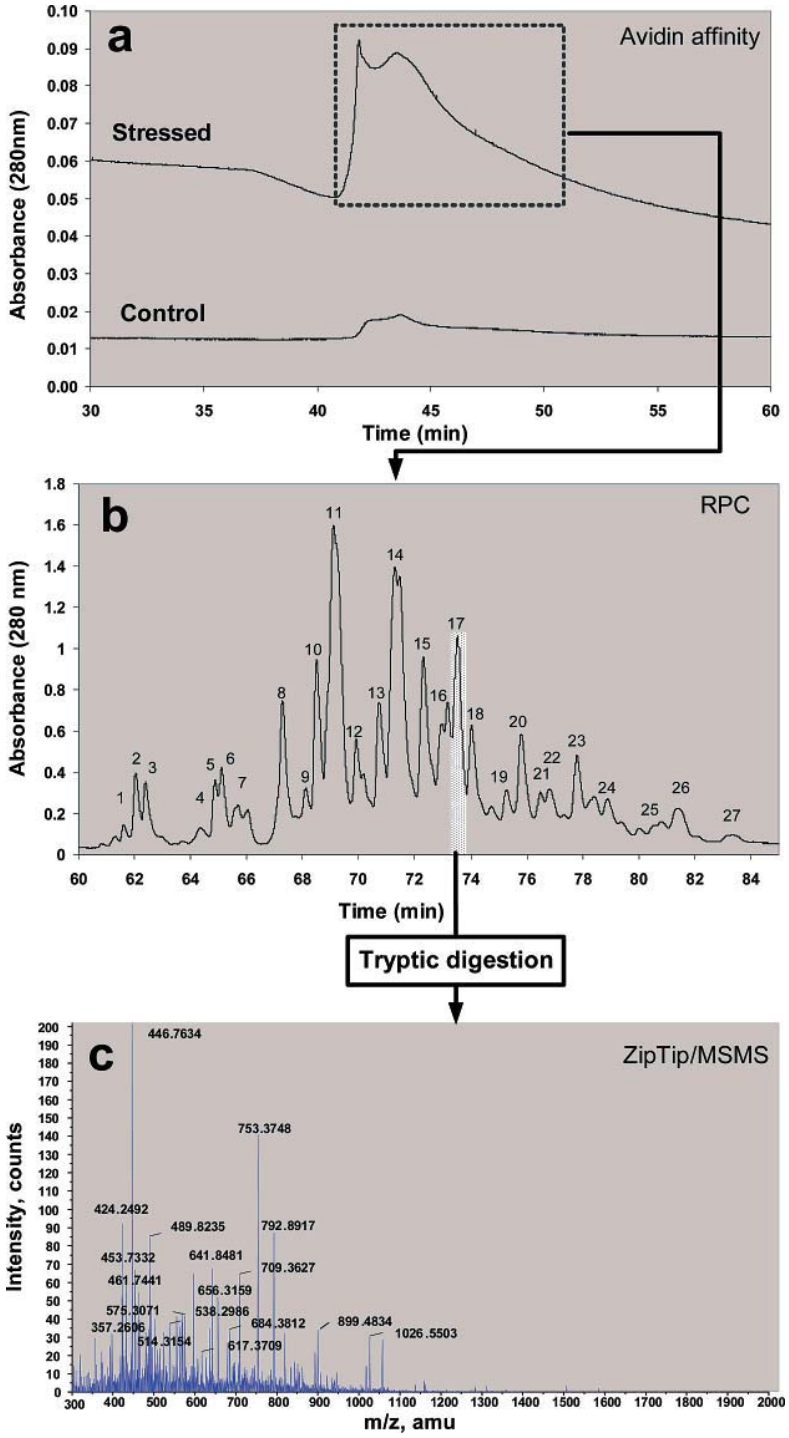

Figure 1. Initial analytical scheme devised for identification of yeast carbonylated proteins. (a) Stressed yeast lysate after biotin hydrazide labeling separated on avidin affinity column (top trace). (b) Avidin selected proteins separated on C_8 RPC column. (c) Fractions collected from C_8 column tryptic digested, analyzed via ZipTip/MS/MS.

number includes different charge states of a peptide, modified and unmodified forms of the same peptide, and all the peptides that were identified in several fractions. A total of 716 distinct peptides were identified from the 66 proteins with an average of 11 peptides per protein. Biotinylation sites were identified in eight of the ribosomal proteins while other oxidation sites were identified in nine more. In all, ribosomal proteins were detected 163 times. Identified ribosomal proteins with their specific name, NCBI gi#, peptide sequence, MASCOT score, and sequence coverage are provided as tables in Supporting Information. Ribosomal proteins with identified oxidation sites are also provided in a separate table including the specific sites of oxidation in addition to all other information mentioned above.

Some proteins were damaged more than others. The severity of oxidation is indicated by the fact that multiple oxidation sites

were noted in the same protein in some cases. Eleven ribosomal proteins were seen to have been modified at a single site while an additional 47 were not found to be oxidatively modified at all. The biotinylation site in these proteins was either not observed or they were selected by the avidin column because they were in some way associated with another protein that was biotinylated. Because the avidin affinity column was eluted with nondenaturing PBS buffer, noncovalently associated proteins can remain bound to biotinylated proteins during affinity chromatography.

Behavior of Ribosomal Proteins during Reversed-Phase Chromatography. One of the striking features of ribosomal proteins observed in this study was the fact that protein pairs would frequently appear in multiple RPC column fractions. In 12 cases, ribosomal proteins were identified in nonadjacent fractions (The data table showing a comprehensive ribosomal protein elution profile is available in Supporting Information). Because the mobile phase used to elute the RPC column dissociates most noncovalently associated protein complexes, there is the strong implication that these coeluting proteins were covalently linked. The fact that protein pairs appeared in more than one fraction suggests they are chromatographing together in multiple forms.

Potential Mechanisms for the Observed Protein−Protein Association To Occur. Protein pairs that coeluted in multiple nonadjacent fractions were grouped in five distinct groups. Assuming that the chromatographic behavior noted above is the result of covalent coupling and that direct cross-linking of these proteins was most likely to occur when they are adjacent in the cell, the position of these protein pairs in the ribosomal assembly was examined. The ribosomal 80s-Eef2-Sordarin complex from yeast obtained by docking atomic models of RNA and protein components in an 11.7 Å Cryo-Em map was used to locate protein pairs in the ribosomal assembly (Figure 2). BLAST searches were used to find the homologues of ribosomal proteins among ribosomal chains composing the complex. In Figure 2a, three ribosomal proteins comprising group number one of cross-linked proteins are represented by chain 9 (homologous to gi|6322554), V (gi|132847), and W (gi|6320128). Of six ribosomal proteins plotted in this group, the position of only three was found in the ribosome assembly. These were chain 9 of the ribosomal 80s-Eef2-Sordarin complex from yeast (60S subunit)), chain V of the complex from yeast (60S subunit)), and chain W of the complex from yeast (60S subunit)). In the 3-D structure of the 60S ribosomal subunit shown in Figure 2a, these proteins are not adjacent, and direct cross-linking as a result of oxidation would seem to be impossible. These proteins are so far apart in the ribosomal matrix that even with the best positioning of the candidates, direct cross-linking seems unlikely.

Group number 3 includes four possibly cross-linked proteins. Two of the four proteins, chain B of the ribosomal 80s-Eef2-Sordarin complex (60S subunit) homologous to gi|596086 and Chain Q of the ribosomal complex (60S subunit) homologous to gi|6319668, were found in the ribosomal protein assembly (Figure 2b). Again, these proteins are separated by a substantial distance. Direct cross-linking of these proteins while in the ribosomal matrix would seem to be unlikely as well.

Group number 5 includes three possibly cross-linked proteins. These include chain T of the ribosomal 80s-Eef2-Sordarin complex (60S subunit) homologous to gi|6324445 and chain R of the complex (60S subunit)) (gi|6319384). They also are separated by sufficient distance to make direct protein−protein cross-linking seem unlikely (figure not shown).

This leads to the conclusion that cross-linking must be occurring by some other mechanism. The single common structural feature between all these proteins is ribosomal RNA (Figure 2c and 2d). Given that proteins have been shown to covalently couple to bases in DNA, especially in fixed protein−DNA structures such as histones, there is the strong possibility that proteins are cross-linking with rRNA. This would mean that in cases were two proteins appear to be cross-linked it would be because they are both linked to the same segment of rRNA. The fact that ribosomal proteins are in a fixed position relative to rRNA further supports this theory. But the fact that multiple coeluting protein pairs were observed that are potentially cross-linked through rRNA requires that rRNA be cleaved in a number of places before the analyses described above were performed. This could have occurred by enzymatic hydrolysis of rRNA before or after cell lysis.[25−27]

Boronate Affinity Chromatography. Assuming that some of the potential protein−rRNA fragments would have a terminal ribose residue with a vicinal diol, the analytical strategy described in Figure 1 was revised to include boronate affinity chromatography and ribonuclease digestion steps as seen in Figure 3. Boronate columns select vicinol diols as could be found in the terminal ribose residue of degraded RNA (Figure 3b).[28] The broad elution peak from the boronate affinity column results from the time it takes for hydrolysis of the borate ester between the boronate stationary phase and diols in the sample. This affinity selection step would thus capture proteins covalently coupled to RNA during the course of oxidative stress in addition to glycated and glycosylated proteins.

Boronate affinity selected proteins were then fractionated on the Vydac C_8 reversed-phase chromatography (RPC) column (Figure 3c). Fractions collected from the RPC column were tryptic digested, and after inhibition of trypsin using TLCK, fractions were treated with ribonuclease I (*E. coli*). The function of the ribonuclease step is to digest RNA. Ribonuclease I from *E. coli* was used because it has a marked preference for single-stranded RNA. This procedure would leave a single nucleotide attached to the peptide at the point of covalent coupling between a protein and RNA.

Mass Spectral Analysis of Peptides from Double Affinity Selected Proteins. After RPC of the cleavage fragments, peptide−nucleotide conjugates were identified by tandem mass spectrometer (Figure 3d) and a MASCOT database search. As expected, the majority of the proteins identified were ribosomal proteins. (A comprehensive table of identified ribosomal proteins including their name, gi|#, sequence, sequence coverage, MASCOT score, and oxidation sites are provided as Supporting Information). Again single ribosomal proteins were detected in multiple fractions after RPC fractionation (Figure 3c). Coelution of protein pairs in nonadjacent fractions during RPC was also seen again. This further supports the hypothesis that this chromatographic behavior is due to protein−RNA cross-linking.

Proving protein−RNA conjugation was more difficult. In order to identify peptide−nucleotide conjugates by tandem mass spectrometry, the modified amino acids structures have to be known and their new masses specified during MASCOT searches. The fact that *in vitro* protein−RNA and −DNA cross-linking studies had been carried out for the purpose of ribosomal structure elucidation was very useful.[29−33] These studies have shown that cross-linking occurs primarily at

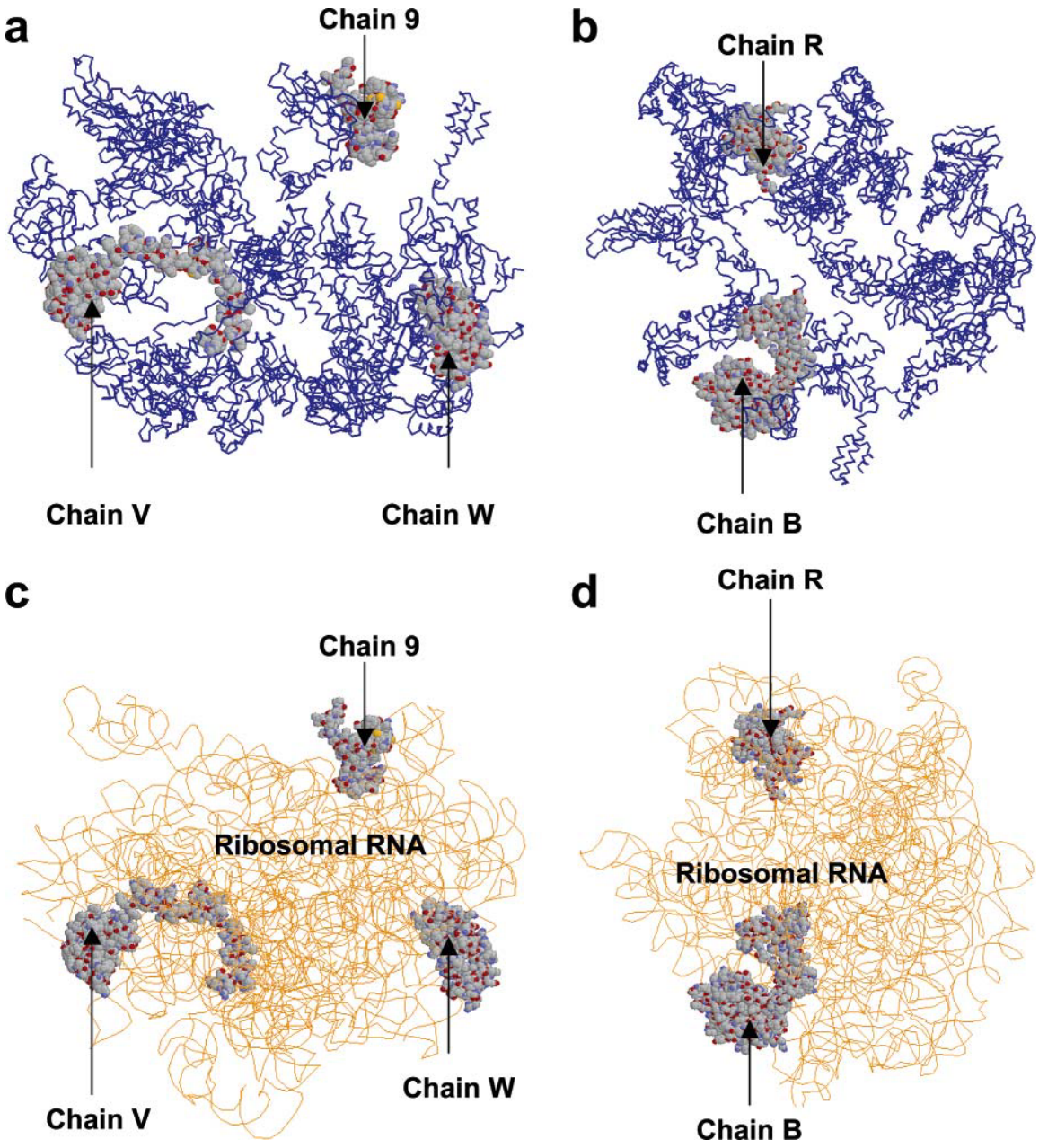

Figure 2. Relative position of ribosomal proteins found in more than one nonadjacent liquid chromatographic fraction (candidate cross-linked proteins). (a) The relative position of chains 9, V, and W of the ribosomal 80s-Eef2-Sordarin complex found simultaneously in fractions no. 7 and 17 does not allow direct cross-linking. (b) Direct cross-linking of chains B and R is also not possible due to the distance separating them. (c) The relative position of rRNA compared to chains 9, V, and W indicates that the only way they could be cross-linking is via rRNA. (d) The position of rRNA relative to chains B and R of the 60S subunit suggests rRNA as a potential cross-linker.

arginine, tyrosine, lysine, serine, and threonine. All these amino acids cross-link to guanine except tyrosine which cross-links to cytosine. Structures of the amino acid−nucleotide conjugates obtained from the literature are provided as Supporting Information. All of these forms of amino acid−nucleotide cross-linking were used in MASCOT database searches as variable modifications. An MS/MS example of a peptide cross-linked to a nucleotide is shown in Figure 4. This peptide (TRAKAKVE-EMNNIIAASR) derived from ribosomal protein L39B (gi|2326843) has two lysine residues cross-linked to guanosine monophosphate at positions 4 and 6 in addition to a sodiated glutamic acid at position 8 and an oxidized methionine at position 10. All of the peptide fragments identified by MASCOT were assigned a label corresponding to their m/z value and their ion type (y or b). The doubly charged b(6) ion ($m/z = 654.73$ Da) and doubly charged b(5) ion ($m/z = 427.67$ Da) clearly showed the presence of a lysine cross-liked to a guanosine monophosphate at position 6 because the mass difference between these two fragments (454.12 Da) matches the mass of a lysine residue carrying a covalently linked guanosine monophosphate residue (Figure 4).

When an amino acid−nucleotide conjugate was identified in the tandem MS data, the accuracy of the identification site was confirmed by noting the position of that amino acid in

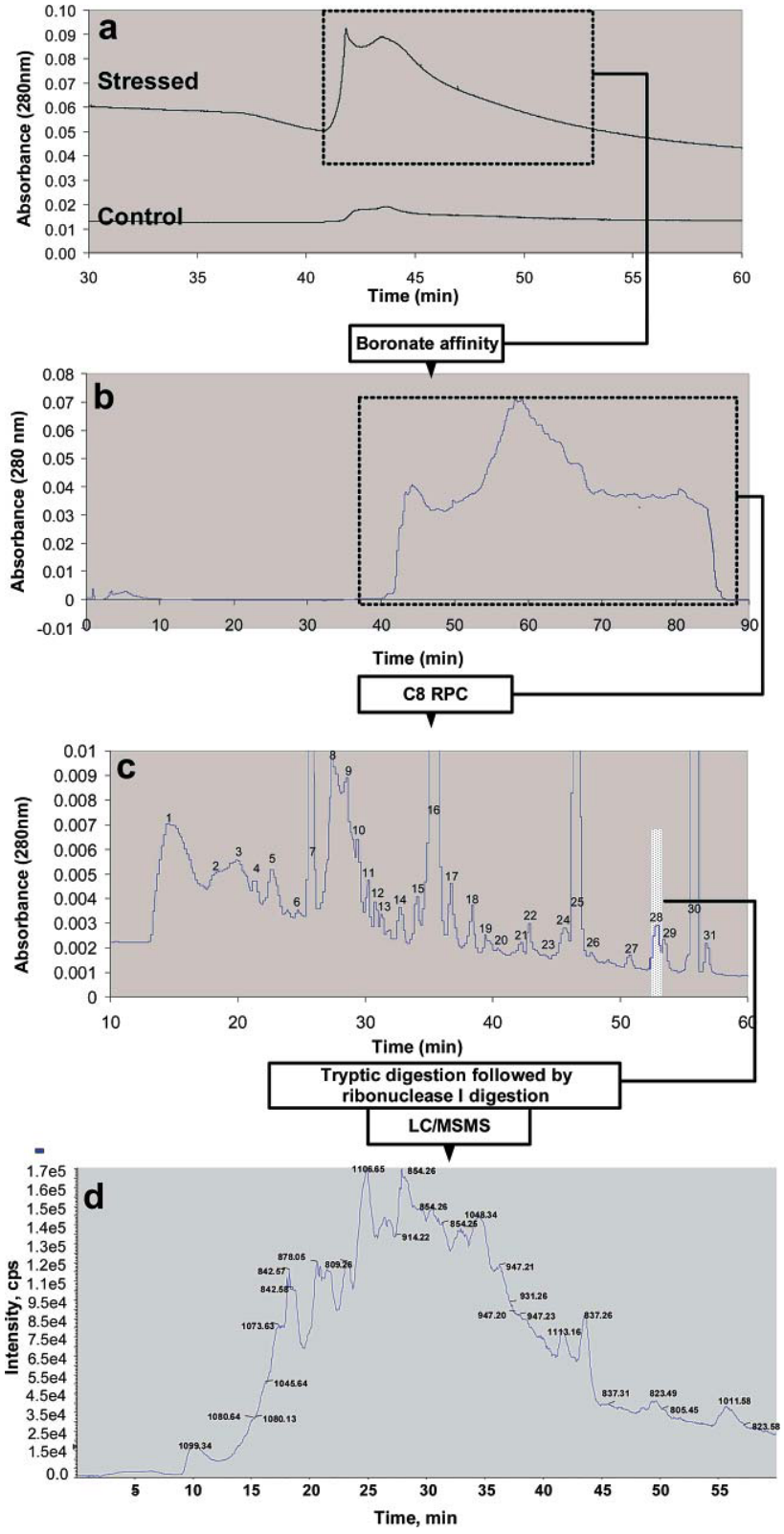

Figure 3. Analytical strategy for isolation of RNA cross-linked proteins. (a) Selection of yeast carbonylated proteins using avidin affinity chromatography. (b) selection of carbonylated proteins which contain vicinal diols using boronate affinity selection. This category may include carbonylated glycoproteins as well as RNA cross-linked carbonylated proteins. (c) C_8-RPC fractionation of avidin-boronate selected proteins. (d) LC/MS/MS analysis of RPC fraction 28 after trypsin digestion of proteins and ribonuclease I digesting of RNA.

the protein relative to the specific identified nucleotide in the 3-D structure of the ribosome. This additional verification was performed due to the higher rate of false positives in searches with large number of variable modifications. Examples are seen

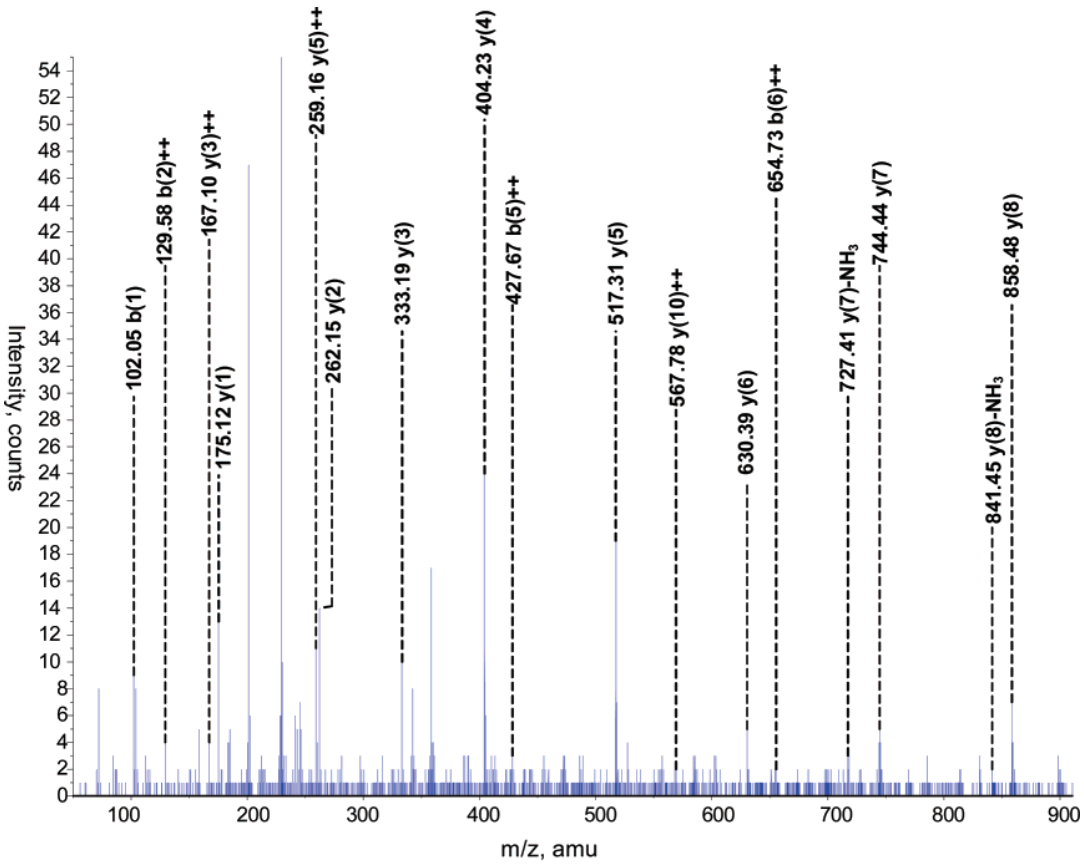

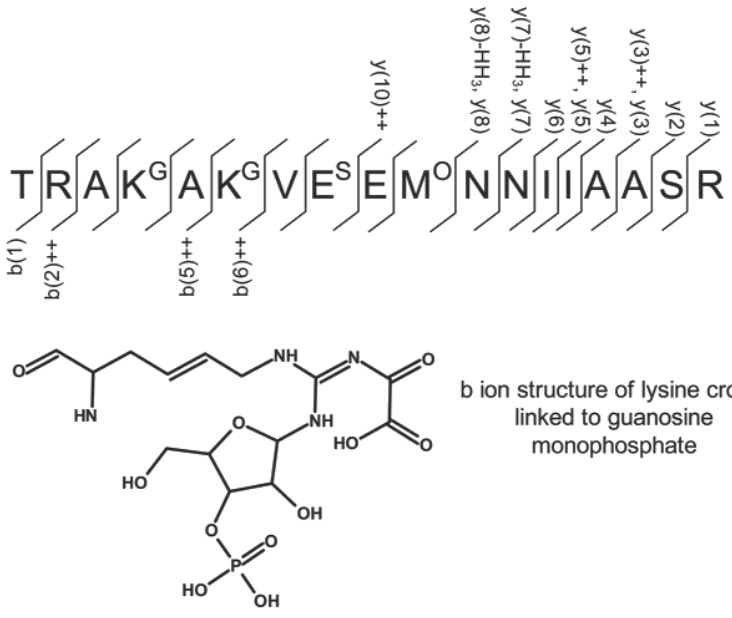

Figure 4. MS/MS analysis of a tryptic peptide from ribosomal protein L39B. (Top) MS/MS spectrum. All of the y and b ions are assigned in the spectrum. (Bottom) Diagram showing the y and b ion map superimposed on the peptide sequence, along with calculation of mass differences. This peptide is cross-linked at both of its lysine to guanosine monophospgate according to the MASCOT identification. Corresponding lysines are superscripted with a G. The oxidized methionine residue is shown with an "O" superscript and sodiated glutamic acid with an "S" superscript in the sequence.

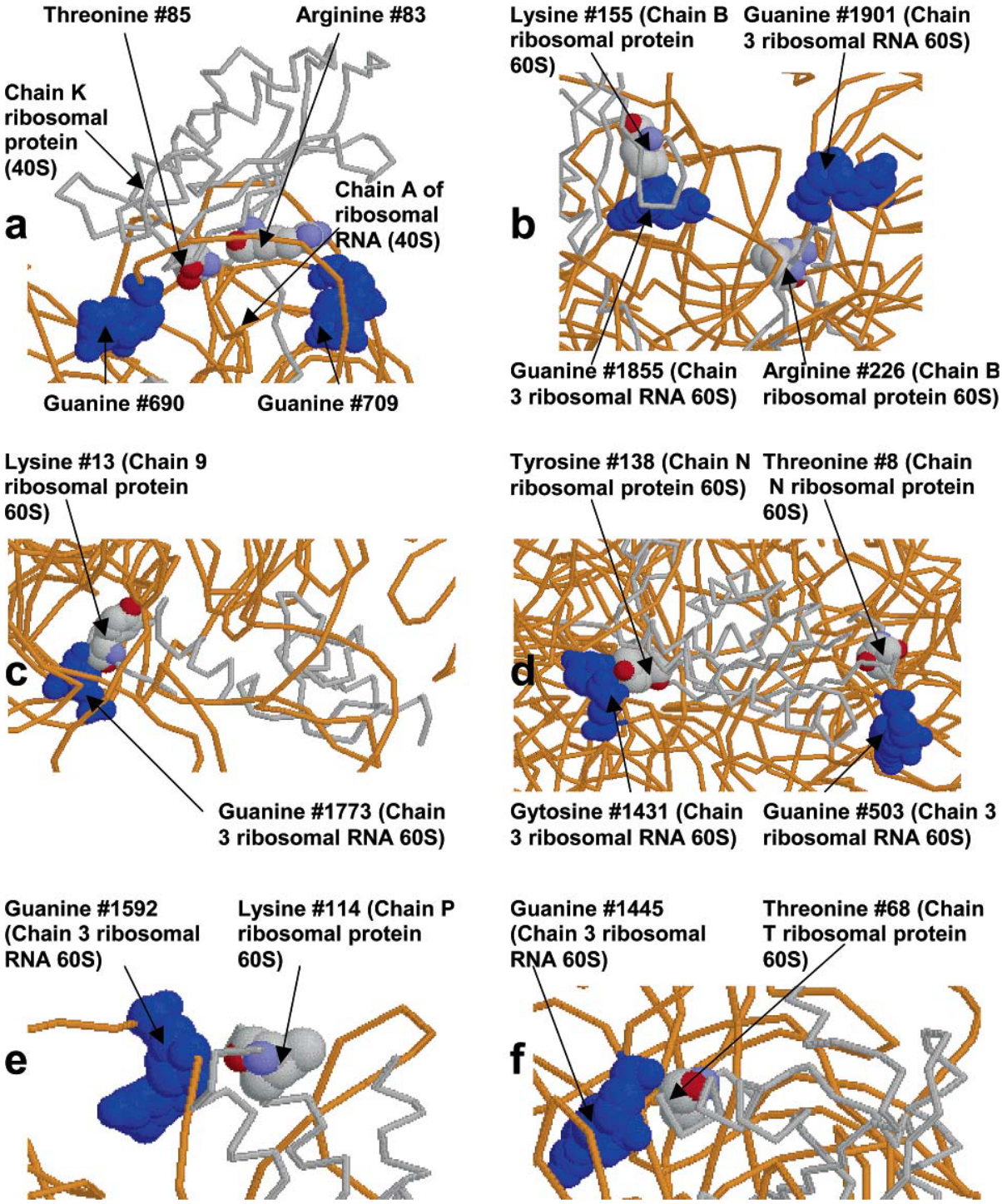

Figure 5. Sites of protein−RNA cross-linking identified by MS/MS. The relative position of the cross-linked amino acids was investigated to confirm that cross-linking is possible, and a candidate nucleotide exists in close proximity to form a covalent bond with the identified amino acid. Candidate nucleotides were found in 90% of the cases. 50% of the amino acids were found to be in direct contact with the candidate nucleotide (b, c, d, and f).

in Figure 5. Chain K of the ribosomal 80s-Eef2-Sordarin complex from the 40S subunit was found in fraction 6 (Figure 3C). On the basis of the MS/MS data, Arg 83 and Thr 85 of this protein are cross-linked to guanine of the ribosomal RNA. The position of the identified amino acids and the proximity of guanines are shown in Figure 5a. The close proximity of Arg 83 and Thr 85 to guanine residues in the ribosomal RNA (Chain A) shows that formation of a protein−RNA conjugate at these sites would be possible. A similar proximity search was performed for other ribosomal proteins with known structure and cross-linking sites. In the case of chain B in the ribosomal 80s-Eef2-Sordarin complex from the 60S subunit, lysine 155 and arginine 226 (Figure 5b) are in close proximity to guanine residues in ribosomal RNA. Guanine residue 1901 was found

in close proximity to the arginine 226, and guanine 1855 was found to be close to lysine 155. When these groups were displayed in a space filling display mode their electron clouds intertwined. Intertwined electron clouds were also found between lysine 13 in chain 9 of the 60S ribosomal subunit and guanine 1773 (Figure 5c), tyrosine 138 in chain N of the 60S ribosomal subunit and cytosine 1431 (Figure 5d), and threonine 68 of chain T in the 60S ribosomal subunit and guanine 1445 (Figure 5f). Also guanine 503 was found in close proximity to threonine 8 of chain N in the 60S ribosomal subunit, and guanine 1592 was found in close proximity to lysine 114 of chain P in the 60S ribosomal subunit.

Discussion

The impact of protein−rRNA cross-linking on biological systems is yet to be determined. The degree to which protein−rRNA cross-linking compromises protein synthesis or increases ribosome degradation is unknown, but it has been observed that ribosomal RNA decreases in yeast cells under oxidative stress.[34] Aging cells are also constantly under attack by ROS. This oxidative damage is cumulative and is believed to trigger cell apoptosis. But the critical details of what type of damage pushes the cell toward suicide are not clear. One of the most important cell functions is the production of proteins to carry on regular tasks. When cells are stressed by ROS, many proteins are damaged and they have to be either repaired or replaced. In either case, special proteins have to be produced in large amounts to carry out these jobs. These facts highlight the critical importance of ribosomes, especially when already impaired aging cells are excessively stressed. RNA oxidation is probably more widespread than previously thought, as has been reported in the case of atherosclerosis.[35] There are also new reports of reduced ribosomal activity in AD. For example a new study shows that in multiple cortical areas of AD subjects, there is a significant impairment in ribosome function that is not observed in the cerebellum of the same subjects. This impairment is linked to a decreased rate and capacity for protein synthesis, decreased ribosomal RNA and tRNA levels, and increased RNA oxidation.[36] It is possible that protein−RNA cross-linking may play a role in early stage ribosomal impairment in AD subjects as well.

Conclusions

On the basis of the data presented here, it is concluded that protein−rRNA complex formation occurs with high frequency during oxidative stress in yeast. From the structures identified by mass spectrometry, it can be further concluded that the mechanism by which protein−rRNA cross-linking occurs does not involve Schiff base formation as is often the case in protein−protein cross-linking. Moreover, on the basis of the similarity of the conjugates identified in these studies to those formed between proteins and DNA, it is concluded that the same free radical mechanism in DNA oxidation is involved in RNA−protein cross-linking. But as yet the exact mechanism is unknown.

Taken together, findings from this study and reports in the literature suggest that (1) covalently cross-linked protein−RNA aggregates form as a result of oxidative stress and (2) this phenomenon has at least some effect on protein expression. The degree to which protein synthesis is compromised, the manner in which protein−RNA conjugates are degraded, and whether protein−RNA aggregates accumulate to a toxic level are yet to be determined. The rate at which microbial cells grow allows them to out-grow problems of this type in many cases. But the problem may be much more serious in mammalian cells that divide slowly as in neurological tissue and the elderly.

Appendix I

1	thereonine oxidized and biotinylated[37,38]
2	proline oxidized and biotinylated[37,39]
3	arginine oxidized and biotinylated[37,40]
4	lysine oxidized and biotinylated[37,41]
5	hydroxylation of histidine and tryptophan[42,43]
6	methionine oxidation[44]
7	histidine oxidation to aspartic acid[45−47]
8	tryptophan oxidation to formylkynurenin[48]
9	tyrosine oxidation to aminotyrosine[49]
10	sodiation of aspartic acid and glutamic acid
11	sodiation at the C terminus
12	cysteine alkylated with iodoacetamide
13	tryptophan oxidation to kynurenin[50]

[a] Modifications in peptides are shown as superscripts for corresponding amino acids in the sequence. Further information regarding mass difference of the modified amino acids can be accessed from Unimod website.

Appendix II

cross-linking	code
tyrosine cross-linked to cytosine[29,30]	α
arginine cross-linked to guanine[31]	β
lysine cross-linked to guanine[32,33]	γ
serine cross-linked to guanine[32,33]	ϵ
threonine cross-linked to guanine[32,33]	ω

[a] Cross-linked type is shown as superscripts for corresponding amino acids in the sequence. Further information regarding mass difference of the modified amino acids can be accessed from references included for each cross-linking.

Acknowledgment. This work was supported by a grant from the National Institutes of Health (1P30- AG13319).

Supporting Information Available: Figure showing the amino acid−nucleotide cross-linked structures; and tables listing the ribosomal proteins (1) for which specific oxidation sites were found, (2) that were identified after avidin affinity selection, and (3) that were identified after double selection with avidin and boronate affinity chromatography. This material is available free of charge via the Internet at http://pubs.acs.org.

References

(1) Solomon, B. Alzheimer's disease and immunotherapy. *Curr. Alzheimer Res.* **2004**, *1* (3), 149−163.
(2) Ames, B. N. Dietary carcinogens and anticarcinogens. Oxygen radicals and degenerative diseases. *Science* **1983**, *221* (4617), 1256−64.
(3) Ames, B. N.; Shigenaga, M. K.; Hagen, T. M. Oxidants, antioxidants, and the degenerative diseases of aging. *Proc. Natl. Acad. Sci. U.S.A.* **1993**, *90* (17), 7915−22.
(4) Shringarpure, R.; Davies, K. J. A. Protein turnover by the proteasome in aging and disease. *Free Radic. Biol. Med.* **2002**, *32* (11), 1084−1089.
(5) Davies, K. J. A. Degradation of oxidized proteins by the 20S proteasome. *Biochimie* **2001**, *83* (3/4), 301−310.
(6) Johansen, M. E.; Muller, J. G.; Xu, X.; Burrows, C. J. Oxidatively Induced DNA-Protein Cross-Linking between Single-Stranded Binding Protein and Oligodeoxynucleotides Containing 8-Oxo-7,8-dihydro-2′-deoxyguanosine. *Biochemistry* **2005**, *44* (15), 5660−5671.
(7) Wang, D.; Kreutzer, D. A.; Essigmann, J. M. Mutagenicity and repair of oxidative DNA damage: insights from studies using defined lesions. *Mutat. Res.* **1998**, *400* (1−2), 99−115.

(8) Davis, S. K.; Bardeen, C. J. Cross-linking of histone proteins to DNA by UV illumination of chromatin stained with Hoechst 33342. *Photochem. Photobiol.* **2003**, *77* (6), 675−679.
(9) Nakano, T.; Terato, H.; Asagoshi, K.; Masaoka, A.; Mukuta, M.; Ohyama, Y.; Suzuki, T.; Makino, K.; Ide, H. DNA-Protein Cross-link Formation Mediated by Oxanine. A Novel Genotoxic Mechanism of Nitric Oxide-Induced DNA Damage. *J. Biol. Chem.* **2003**, *278* (27), 25264−25272.
(10) Dimitrov, S. I.; Moss, T. UV laser-induced protein-DNA crosslinking. *Methods in Molecular Biology*; Totowa, NJ, 2001; Vol. 148 (DNA-Protein Interactions, 2nd ed.), pp 395−402.
(11) Matsumoto, A.; Hanawalt, P. C. Histone H3 and heat shock protein GRP78 are selectively cross-linked to DNA by photoactivated gilvocarcin V in human fibroblasts. *Cancer Res.* **2000**, *60* (14), 3921−3926.
(12) Tiss, A.; Barre, O.; Michaud-Soret, I.; Forest, E. Characterization of the DNA-binding site in the ferric uptake regulator protein from Escherichia coli by UV crosslinking and mass spectrometry. *FEBS Lett.* **2005**, *579* (25), 5454−5460.
(13) Giron-Monzon, L.; Manelyte, L.; Ahrends, R.; Kirsch, D.; Spengler, B.; Friedhoff, P. Mapping Protein-Protein Interactions between MutL and MutH by Cross-linking. *J. Biol. Chem.* **2004**, *279* (47), 49338−49345.
(14) Zheng, Y.; Sheppard, T. L. Half-Life and DNA Strand Scission Products of 2-Deoxyribonolactone Oxidative DNA Damage Lesions. *Chem. Res. Toxicol.* **2004**, *17* (2), 197−207.
(15) Chepanoske, C. L.; Lukianova, O. A.; Lombard, M.; Golinelli-Cohen, M.-P.; David, S. S. A Residue in MutY Important for Catalysis Identified by Photocross-Linking and Mass Spectrometry. *Biochemistry* **2004**, *43* (3), 651−662.
(16) Stadtman, E. R.; Berlett, B. S. Free-radical-mediated modification of proteins. *Free Radical Toxicol.* **1997**, 71−87.
(17) Cohn, J. A.; Tsai, L.; Friguet, B.; Szweda, L. I. Chemical characterization of a protein-4-hydroxy-2-nonenal cross-link: immunochemical detection in mitochondria exposed to oxidative stress. *Arch. Biochem. Biophys.* **1996**, *328* (1), 158−64.
(18) Chen, Q.; Ding, Q.; Keller, J. N. The stationary phase model of aging in yeast for the study of oxidative stress and age-related neurodegeneration. *Biogerontology* **2005**, *6* (1), 1−13.
(19) Potashkin, J. A.; Meredith, G. E. The Role of Oxidative Stress in the Dysregulation of Gene Expression and Protein Metabolism in Neurodegenerative Disease. *Antioxid. Redox Signaling* **2006**, *8* (1, 2), 144−151.
(20) Grune, T.; Jung, T.; Merker, K.; Davies, K. J. A. Decreased proteolysis caused by protein aggregates, inclusion bodies, plaques, lipofuscin, ceroid, and aggresomes during oxidative stress, aging, and disease. *Int. J. Biochem. Cell Biol.* **2004**, *36* (12), 2519−2530.
(21) Schmitt, H. P. Protein ubiquitination, degradation and the proteasome in neuro-degenerative disorders: No clear evidence for a significant pathogenetic role of proteasome failure in Alzheimer disease and related disorders. *Med. Hypoth.* **2006**, *67* (2), 311−317.
(22) Yoo, B.-S.; Regnier, F. E. Proteomic analysis of carbonylated proteins in two-dimensional gel electrophoresis using avidin-fluorescein affinity staining. *Electrophoresis* **2004**, *25* (9), 1334−1341.
(23) Michaelis, S.; Herskowitz, I. The a-factor pheromone of Saccharomyces cerevisiae is essential for mating. *Mol. Cell. Biol.* **1988**, *8* (3), 1309−18.
(24) Mirzaei, H.; Regnier, F. Creation of Allotypic Active Sites during Oxidative Stress. *J. Proteome Res.* **2006**, *5* (9), 2159−2168.
(25) Crawford, D. R.; Lauzon, R. J.; Wang, Y. H.; Mazurkiewicz, J. E.; Schools, G. P.; Davies, K. J. A. 16S mitochondrial ribosomal RNA degradation is associated with apoptosis. *Free Radic. Biol. Med.* **1997**, *22* (7), 1295−1300.
(26) Caldas, T.; Binet, E.; Bouloc, P.; Costa, A.; Desgres, J.; Richarme, G. The FtsJ/RrmJ heat shock protein of *Escherichia coli* is a 23 S ribosomal RNA methyltransferase. *J. Biol. Chem.* **2000**, *275* (22), 16414−16419.
(27) Wilk, H. E.; Kecskemethy, N.; Schafer, K. P. M-Aminophenylboronate Agarose Specifically Binds Capped Snrna and Messenger-Rna. *Nucleic Acids Res.* **1982**, *10* (23), 7621−7633.
(28) Liu, X.-C.; Scouten, W. H. Boronate affinity chromatography. *Methods in Molecular Biology*; Totowa, NJ, 2000; Vol. 147 (Affinity Chromatography), pp 119−128.
(29) Olinski, R.; Nackerdien, Z.; Dizdaroglu, M. DNA-protein crosslinking between thymine and tyrosine in chromatin of g-irradiated or hydrogen peroxide-treated cultured human cells. *Arch. Biochem. Biophys.* **1992**, *297* (1), 139−43.
(30) Ban, F.; Lundqvist, M. J.; Boyd, R. J.; Eriksson, L. A. Theoretical Studies of the Cross-Linking Mechanisms between Cytosine and Tyrosine. *J. Am. Chem. Soc.* **2002**, *124* (11), 2753−2761.
(31) Nguyen, K. L.; Steryo, M.; Kurbanyan, K.; Nowitzki, K. M.; Butterfield, S. M.; Ward, S. R.; Stemp, E. D. A. DNA-Protein Cross-Linking from Oxidation of Guanine via the Flash-Quench Technique. *J. Am. Chem. Soc.* **2000**, *122* (15), 3585−3594.
(32) Morin, B.; Cadet, J. Benzophenone photosensitization of 2′-deoxyguanosine: characterization of the 2R and 2S diastereoisomers of 1-(2-deoxy-beta-D-erythro-pentofuranosyl)- 2-methoxy-4,5-imidazolidinedione. A model system for the investigation of photosensitized formation of DNA-protein crosslinks. *Photochem. Photobiol.* **1994**, *60* (2), 102−9.
(33) Morin, B.; Cadet, J. Type I benzophenone-mediated nucleophilic reaction of 5′-amino-2′,5′-dideoxyguanosine. A model system for the investigation of photosensitized formation of DNA-protein cross-links. *Chem. Res. Toxicol.* **1995**, *8* (5), 792−9.
(34) Crawford, D. R.; Lauzon, R. J.; Wang, Y.; Mazurkiewicz, J. E.; Schools, G. P.; Davies, K. J. A. 16S mitochondrial ribosomal RNA degradation is associated with apoptosis. *Free Radic. Biol. Med.* **1997**, *22* (7), 1295−1300.
(35) Martinet, W.; De Meyer, G. R. Y.; Herman, A. G.; Kockx, M. M. Reactive oxygen species induce RNA damage in human atherosclerosis. *Eur. J. Clin. Invest.* **2004**, *34* (5), 323−327.
(36) Ding, Q.; Markesbery, W. R.; Chen, Q.; Li, F.; Keller, J. N. Ribosome Dysfunction Is an Early Event in Alzheimer's Disease. *J. Neurosci.* **2005**, *25* (40), 9171−9175.
(37) Mirzaei, H.; Regnier, F. Affinity chromatographic selection of carbonylated proteins followed by identification of oxidation sites using tandem mass spectrometry. *Anal. Chem.* **2005**, *77* (8), 2386−2392.
(38) Amici, A.; Levine, R. L.; Tsai, L.; Stadtman, E. R. Conversion of amino acid residues in proteins and amino acid homopolymers to carbonyl derivatives by metal-catalyzed oxidation reactions. *J. Biol. Chem.* **1989**, *264* (6), 3341−6.
(39) Taborsky, G.; McCollum, K. Oxidative modification of proteins in the presence of ferrous ion and air. Effect of ionic constituents of the reaction medium on the nature of the oxidation products. *Biochemistry* **1973**, *12* (7), 1341−8.
(40) Creeth, J. M.; Cooper, B.; Donald, A. S. R.; Clamp, J. R. Studies of the limited degradation of mucus glycoproteins. The effect of dilute hydrogen peroxide. *Biochem. J.* **1983**, *211* (2), 323−32.
(41) Requena, J. R.; Chao, C.-C.; Levine, R. L.; Stadtman, E. R. Glutamic and aminoadipic semialdehydes are the main carbonyl products of metal-catalyzed oxidation of proteins. *Proc. Natl. Acad. Sci. U.S.A.* **2001**, *98* (1), 69−74.
(42) Maskos, Z.; Rush, J. D.; Koppenol, W. H. The Hydroxylation of Tryptophan. *Arch. Biochem. Biophys.* **1992**, *296* (2), 514−520.
(43) Guptasarma, P.; Balasubramanian, D.; Matsugo, S.; Saito, I. Hydroxyl Radical Mediated Damage to Proteins, with Special Reference to the Crystallins. *Biochemistry* **1992**, *31* (17), 4296−4303.
(44) Manneberg, M.; Lahm, H. W.; Fountoulakis, M. Oxidation of Cysteine and Methionine Residues During Acid-Hydrolysis of Proteins in the Presence of Sodium-Azide. *Anal. Biochem.* **1995**, *224* (1), 122−127.
(45) Berlett, B. S.; Levine, R. L.; Stadtman, E. R. Comparison of the effects of ozone on the modification of amino acid residues in glutamine synthetase and bovine serum albumin. *J. Biol. Chem.* **1996**, *271* (8), 4177−82.
(46) Uchida, K.; Kawakishi, S. 2-Oxohistidine as a novel biological marker for oxidatively modified proteins. *FEBS Lett.* **1993**, *332* (3), 208−10.
(47) Farber, J. M.; Levine, R. L. Sequence of a peptide susceptible to mixed-function oxidation. Probable cation binding site in glutamine synthetase. *J. Biol. Chem.* **1986**, *261* (10), 4574−8.
(48) Armstron Rc; Swallow, A. J. Pulse-Radiolysis and Gamma-Radiolysis of Aqueous Solutions of Tryptophan. *Radiat. Res.* **1969**, *40* (3), 563−&.
(49) Kikugawa, K.; Kato, T.; Okamoto, Y. Damage of amino acids and proteins induced by nitrogen dioxide, a free radical toxin, in air. *Free Radic. Biol. Med.* **1994**, *16* (3), 373−82.
(50) Pryor, W. A.; Uppu, R. M. A kinetic model for the competitive reactions of ozone with amino acid residues in proteins in reverse micelles. *J. Biol. Chem.* **1993**, *268* (5), 3120−6.

PR060337L